Pinning-Dependent Field-Driven Domain Wall Dynamics and Thermal Scaling in an Ultrathin Pt/Co/Pt Magnetic Film

J. Gorchon,[1] S. Bustingorry,[2] J. Ferré,[1] V. Jeudy,[1,3,*] A. B. Kolton,[2] and T. Giamarchi[4]

[1]*Laboratoire de Physique des Solides, Université Paris-Sud, CNRS, UMR8502, 91405 Orsay, France*
[2]*CONICET, Centro Atómico Bariloche, 8400 San Carlos de Bariloche, Río Negro, Argentina*
[3]*Université Cergy-Pontoise, 95000 Cergy-Pontoise, France*
[4]*DPMC-MaNEP, University of Geneva, 24 Quai Ernest Ansermet, CH-1211 Geneva, Switzerland*

Magnetic-field-driven domain wall motion in an ultrathin Pt/Co(0.45 nm)/Pt ferromagnetic film with perpendicular anisotropy is studied over a wide temperature range. Three different pinning dependent dynamical regimes are clearly identified: the creep, the thermally assisted flux flow, and the depinning, as well as their corresponding crossovers. The wall elastic energy and microscopic parameters characterizing the pinning are determined. Both the extracted thermal rounding exponent at the depinning transition, $\psi = 0.15$, and the Larkin length crossover exponent, $\phi = 0.24$, fit well with the numerical predictions.

Many areas in physics [1–8] such as magnetic and ferroelectric domain-wall motion, contact lines in wetting, crack propagation, vortex lines motion in type-II superconductors, etc., involve the displacement of elastic object or interface in a weakly disordered medium. How the velocity of motion depends on the driving force f poses important fundamental questions [1,2,5,6]. In the absence of disorder or for a large f, motion is limited by dissipation and the interface moves in a flow regime, with a velocity essentially proportional to f. However in real materials the presence of disorder leads to pinning which dramatically modifies the response to the force. At zero temperature this leads to the existence of a depinning force $f_{\rm dep}$, below which no motion takes place. At finite temperature T the combination of the applied force, collective pinning, and thermal effects leads to an extremely rich dynamical behavior, which has been the focuss of many theoretical [1,2,5,6,9] and experimental studies [10–16].

On the experimental front the controlled investigation of this dynamics is very difficult and Pt/Co/Pt ultrathin ferromagnetic films with perpendicular anisotropy proved to be an archetypal 2D-disordered system to test theory [10,13,16–19]. In this system the force f is the applied field H, and domain walls (DWs) mimic elastic interfaces. Measurements as a function of the field, allow us to unambiguously evidence the highly nonlinear response $\ln v(H) \sim H^{-\mu}$ expected at small fields, the so called creep regime [10,16,17]. They confirm the predicted value $\mu = 1/4$ of the exponent and its relation with the exponent associated to the roughness of the interface at equilibrium [1,4,7,10]. Measurements as a function of the temperature [20,21] for small fields, confirm the role played by thermal activation over barriers by obtaining a prefactor in the exponential varying as $1/T$.

At larger fields, and in particular close to the depinning transition, the situation, both theoretically and experimentally, is much less clear. At the depinning field $H_{\rm dep}$ the response was predicted to follow a power law behavior, $v(H_{\rm dep}) \sim T^{\psi}$, where ψ is the thermal rounding exponent [5]. This behavior was checked indirectly [22] in experiments with a constant T but with Pt/Co/Pt layers of different anisotropy. However, a true temperature dependent analysis close to depinning is still lacking, as well as bridging the gap between the very low field creep regime $H \ll H_{\rm dep}$ and the depinning one $H \sim H_{\rm dep}$. For this, experiments with a full range of magnetic fields and various temperature is necessary.

In this Letter, we perform such a study by exploring in a single Pt/Co/Pt ultrathin layer the DW dynamics between 50 and 300 K. We evidence three distinct pinning dependent regimes and determine the corresponding crossover fields. We provide a consistent theoretical description of the full dynamical range, allowing us in addition, through the testing of the predicted universal scalings, to obtain accurately the (nonuniversal) microscopic quantities controlling DW dynamics.

The experimental results were obtained with a sputtergrown ultrathin Pt(3.5 nm)/Co(0.45 nm)/Pt(4.5 nm) film deposited on an etched Si/SiO$_2$ substrate [16]. The Curie temperature ($T_C = 375$ K), square perpendicular hysteresis loop, thermal dependence of the saturated magnetization—compatible with that predicted for an anisotropic 2D-ferromagnet—and of the anisotropy field, were determined from magnetooptical Kerr magnetometry and microscopy measurements [23]. The film was cooled in an open cycle optical cryostat and its temperature was measured with an accuracy of ± 2 K. The DW motion was produced by field pulses and visualized by Kerr microscopy with a resolution of ~ 1 μm. The DW velocity, $v(H)$, was deduced from the
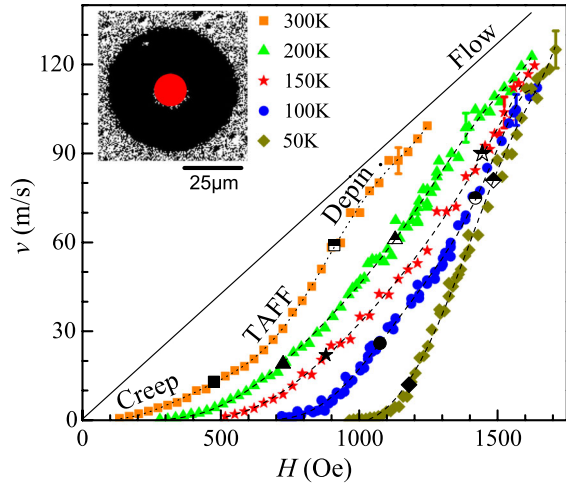
FIG. 1 (color online). Variation of the domain wall velocity in the Pt/Co(0.45 nm)/Pt film with H for different temperatures. The big black filled and half-filled symbols correspond to boundaries between the creep and TAFF regimes, $H_{C\text{-}T}$, and TAFF and *depinning* regimes, H_{dep}, respectively. The straight line represents the predicted asymptotic high-field *flow* limit at 300 K for $m = 0.085$ m/s Oe. Inset: Domain wall displacement (in black) from a nucleus (in red) produced by a 1 μs field pulse of amplitude $H = 865$ Oe, at 150 K.

growth in diameter of magnetically reversed bubbles (Fig. 1, inset). The field pulses ($0 < H < 1600$ Oe) were produced by a 60-turn small coil (0.16 μs rise time) positioned very close to the film surface [23]. For each pulse amplitude and duration (from 0.5 μs to 100 μs), the DW displacements were analyzed in order to select only steady DW motion.

The DW velocity $v(H)$ curves are depicted in Fig. 1, for temperatures ranging between 50 and 300 K. The main parameters controlling DW motion are reported in Table I. As it can be observed, lowering the temperature results in a shift towards the high-field region of the curves. Different dynamical regimes when raising the applied magnetic field H are indicated in Fig. 1 on the highest temperature (300 K) curve. Their precise identification is not straightforward and will be discussed in detail below. The high-field $v(H)$

response is supposed to finally reach the asymptotic *flow* regime with a mobility $m = v/H$ (as shown in Fig. 1) [16]. Unfortunately, the determination of v for $H > 1700$ Oe was not possible due to the increase of the nucleation rate of magnetization reversal [23]. The value of m (reported in Table I) is then determined from the expected power law expression [24], $m - (v/H) = DH^{-c}$ with $c = 4$. A small increase of m is revealed when lowering the temperature [23].

Let us now identify the low field regimes in detail. Two different behaviors for the velocity can be clearly seen in Fig. 2. At lower fields $\ln v$ exhibits a linear variation with $H^{-1/4}$ and this part can be identified with the creep regime, in which the barriers diverge for $H \to 0$ [1,25,26]. In this regime, the DW velocity can be written

$$v_{\text{creep}}(H,T) = v^0_{\text{creep}}(T)e^{-(T_{\text{dep}}/T)(H_{\text{dep}}/H)^\mu}, \quad (1)$$

where v^0_{creep} corresponds to a velocity prefactor whose meaning is discussed later, and T_{dep} is the depinning temperature which is defined below. As observed in Fig. 2(a), the creep law is no longer fulfilled at high (low) H values ($H^{-1/4}$-values) and a new regime of transport can be identified above the field $H_{C\text{-}T}$ (creep), given in Table I and which corresponds to the upper boundary of the creep regime.

For $H \geq H_{C\text{-}T}$ (creep), $\ln v$ varies linearly with H, as shown in Fig. 2(b). The experiment thus reveals a regime in which the barriers decrease linearly as the field is increased and the velocity obeys

$$v_{\text{TAFF}}(H,T) = v^0_{\text{TAFF}}(T)e^{-(T_{\text{dep}}/T)[1-(H/H_{\text{dep}})]}, \quad (2)$$

where $v^0_{\text{TAFF}}(T)$ is the velocity at $H = H_{\text{dep}}$. This regime can be identified with the so-called thermally assisted flux flow (TAFF) regime [27] initially proposed in the context of vortex motion and is compatible with the computed behavior in a $T = 0^+$ dynamics [6]. As shown in Fig. 2(b), the limits of the TAFF regime ($\ln v \sim H$) permit us to obtain $H_{C\text{-}T}$(TAFF) and the depinning threshold, H_{dep}(TAFF), reported in Table I. More strictly, the end of

TABLE I. Parameters controlling DW dynamics at different temperatures. M_s is the magnetization saturation and m the DW mobility in the *flow* regime [23]. Between the field boundaries $H_{C\text{-}T}$ and H_{dep}, DWs follow a thermally assisted flux flow (TAFF) regime. The two sets of $H_{C\text{-}T}$ and H_{dep} values were determined by independent methods (see text) and are consistent together. The T_{dep} value was deduced from the creep regime data.

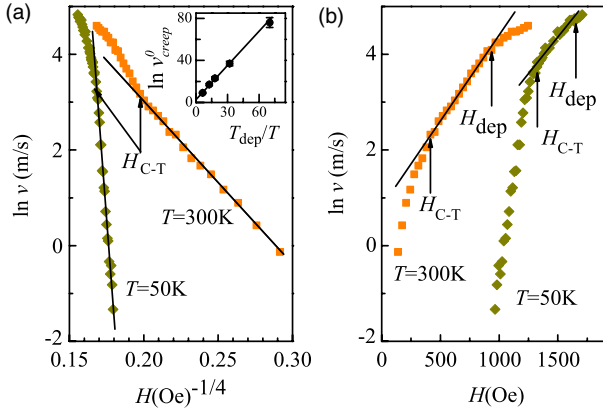| T (K)	300	200	150	100	50
M_s (erg/G cm^3)	800(40)	1120(50)	1260(60)	1370(70)	1470(80)
m (m/s Oe)	0.085(0.04)	0.083(0.05)	0.091(0.05)	0.089(0.06)	0.102(0.07)
$H_{C\text{-}T}$ (creep) (Oe)	480(20)	720(30)	870(40)	1080(40)	1170(40)
$H_{C\text{-}T}$ (TAFF) (Oe)	470(20)	730(30)	890(40)	1070(40)	1190(40)
H_{dep} (TAFF) (Oe)	920(30)	1060(50)	1360(30)	1480(50)	1500(40)
H_{dep} (depin.) (Oe)	900(40)	1190(40)	1335(50)	1360(50)	1470(50)
T_{dep} (K)	1880(110)	2500(150)	2700(160)	3200(190)	3500(210)

FIG. 2 (color online). Field-dependent domain wall velocity. (a) Plot of $\ln v$ vs $H^{-1/4}$ to evidence the creep regime and its upper boundary $H_{C\text{-}T}$ (creep). Inset: creep prefactor v_{creep}^0 deduced from an extrapolation of the creep law (straight line) to $H^{-1/4} = 0$. (b) Plot of $\ln v$ vs H reveals the TAFF regime and its two boundaries $H_{C\text{-}T}$ (TAFF) and H_{dep} (TAFF).

the TAFF regime corresponds to the field $(H \sim H_{\mathrm{dep}}(1 - T/T_{\mathrm{dep}}) < H_{\mathrm{dep}})$ at which the barrier is of the order of the temperature, and at small temperature this field is expected to approach H_{dep}.

Beyond H_{dep} the system enters in the depinning regime for which the velocity is expected to follow the universal scaling form [5,24,28–30]:

$$v_{\mathrm{dep}}(H, T) = v_{\mathrm{dep}}^0(T) G\left[\frac{H - H_{\mathrm{dep}}}{H_{\mathrm{dep}}} \left(\frac{T}{T_{\mathrm{dep}}} \right)^{-\psi/\beta} \right] \quad (3)$$

where $G(x)$ is a universal function such that $G(x) \sim x^\beta$ for $x \gg 1$, i.e., $T \ll T_{\mathrm{dep}}$, with β the depinning exponent, and $v_{\mathrm{dep}}^0 = v_{\mathrm{dep}}(H = H_{\mathrm{dep}}, T) = m H_{\mathrm{dep}}(T/T_{\mathrm{dep}})^\psi$, with ψ the thermal rounding exponent. Thus, the velocity scaling in the depinning regime provides an alternative for estimating H_{dep} [23], according to the procedure proposed in Ref. [22], by considering that the DW velocity fits a $v \sim (H - H_{\mathrm{dep}})^\beta$ law, where $\beta = 0.25$ [31]. This procedure leads to H_{dep}(depin.) in Table I. Knowing H_{dep}, the values for T_{dep} reported in Table I were deduced from the creep plot slope, $T_{\mathrm{dep}} H_{\mathrm{dep}}^{1/4}/T$. Note that the different estimation methods lead to consistent values for $H_{C\text{-}T}$ and H_{dep}, with $H_{C\text{-}T} = 0.5$–$0.8\ H_{\mathrm{dep}}$, as shown in Table I.

The theoretical analysis of the data thus provides a consistent picture of *all* the regimes. Their matching allows us to extract additional results. We in particular analyze the temperature variation of the creep velocity prefactor v_{creep}^0 [cf. Eq. (1)], shown in the inset of Fig. 2(a). The values of $\ln v_{\mathrm{creep}}^0$ are deduced from the extrapolation to $H^{-1/4} = 0$ of the creep plot of Fig. 2(a). Empirically, the velocity v_{creep}^0 is found to fit well with an exponential variation $v_{\mathrm{creep}}^0 = v_{\mathrm{creep}}'^0 \exp(C T_{\mathrm{dep}}/T)$, over the explored temperature range $T/T_{\mathrm{dep}} = 0.014$ to 0.160. The best fit gives $C = 1.04 \pm 0.02$ and $v_{\mathrm{creep}}'^0 = 35 \pm 15\ m/s$. This strongly

suggests that the velocity $v_{\mathrm{creep}}'^0$ must be written as $v_{\mathrm{creep}}'^0 = \xi/\tau$, where ξ is the disorder correlation length, and $1/\tau$ the attempt frequency at passing barriers. Note that such a temperature dependent prefactor simply corresponds, in the creep regime, to a subdominant correction of the barrier. Extracting the explicit temperature dependence allows us to obtain the microscopic attempt frequency. Since $\xi \approx 19$ nm (to be discussed below), one obtains a reasonable time scale of $\tau \approx 1$ ns. Using this exponential behavior of v_{creep}^0 and matching the creep and TAFF velocities at the crossover field $H_{C\text{-}T}$, a value of $C = 0.66 \pm 0.08$ can be obtained, which is of the same order of magnitude and almost temperature independent, as the previously extracted C value.

The crossover between the TAFF and depinning is also consistent with the expected thermal rounding of the velocity in the depinning regime. Matching the TAFF and the depinning regime at H_{dep}, the prefactor in Eq. (2) should be $v_{\mathrm{TAFF}}^0 = v_{\mathrm{dep}}(H = H_{\mathrm{dep}}, T)$, allowing us to use the velocity corresponding to the upper bound of the TAFF regime to extract the thermal rounding exponent ψ. As shown in Fig. 3, the values are consistent with the prediction ($\psi = 0.15$) of numerical simulations based on the quenched-Edwards-Wilkinson equation describing the overdamped motion of an elastic interface in a weak quenched disorder [5].

In order to complete this analysis of universal exponents (i.e., the universality class) we now determine the nonuniversal (intrinsic) characteristic length and energy scales controlling the pinning and their temperature dependence. The free energy, $F(L, u)$, of a DW segment of length L, displaced over a distance u under the action of the magnetic field writes as

$$F(L, u) = \epsilon_{\mathrm{el}} u^2/L - \epsilon_{\mathrm{pin}} u \sqrt{n_i \Delta L} - M_s H t L u, \quad (4)$$
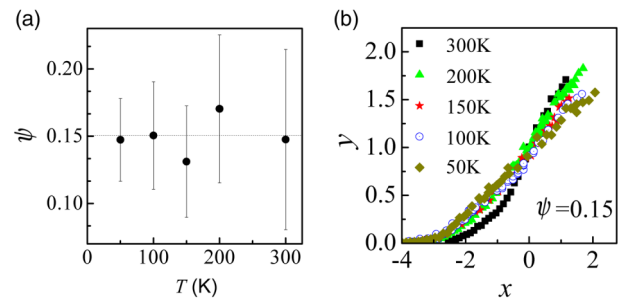

FIG. 3 (color online). (a) ψ as a function of T calculated from the crossover at $H = H_{\mathrm{dep}}$ between the TAFF and thermal rounding regimes, $v_{\mathrm{TAFF}}^0/(m H_{\mathrm{dep}}) = (T/T_{\mathrm{dep}})^\psi$. (b) Universal scaling plot of the depinning transition using $\psi = 0.15$, $\beta = 0.25$ and the parameters of Table I. With the reduced coordinates $x = [(H - H_{\mathrm{dep}})/H_{\mathrm{dep}}](T/T_{\mathrm{dep}})^{-\psi/\beta}$ and $y = [v/(m H_{\mathrm{dep}})](T/T_{\mathrm{dep}})^{-\psi}$, the velocity curves (cf. Fig. 1) are superimposed in the vicinity of the depinning transition ($x = 0$), as expected from Eq. (3).

where n_i is the density of pinning centers assumed to be equal to $1/\xi^2$. M_s is the measured magnetization at saturation (Table I), $t = 0.45$ nm the Co layer thickness, and $\Delta = \sqrt{A/K_{\text{eff}}}$ the DW thickness parameter. The first term in Eq. (4) represents the elastic energy of the wall, F_{el}, the second is the pinning energy, F_{pin}, while the third term stands for the Zeeman contribution, F_H. From this free energy we can derive expressions for the fundamental energy and length scales. In particular, the Larkin length, i.e., the length scale below which elasticity dominates over disorder, has direct experimental relevance [13]. The Larkin length, L_c, which is supposed to be larger than ξ, and the depinning field, H_{dep}, can be defined from the equalities $F_{\text{el}}(L_c, \xi) = F_{\text{pin}}(L_c, \xi)$ and $F_{\text{el}}(L_c, \xi) = F_H(L_c, \xi)$.

Assuming that $k_B T_{\text{dep}} = F_{\text{pin}}(L_c, \xi)(= \epsilon_{\text{pin}}\sqrt{\Delta L_c})$, the following expressions hold:

$$\epsilon_{\text{el}} = (k_B T_{\text{dep}})^2/(M_s H_{\text{dep}} t)\xi^3, \qquad (5)$$

$$\epsilon_{\text{pin}}^2 = [(k_B T_{\text{dep}})(M_s H_{\text{dep}} t)\xi]/\Delta, \qquad (6)$$

$$L_c = (k_B T_{\text{dep}})/[(M_s H_{\text{dep}} t)\xi]. \qquad (7)$$

The DW elastic energy density is expressed as $\epsilon_{\text{el}} = 4t\sqrt{AK_{\text{eff}}}$. The estimated values of the exchange stiffness A and the effective anisotropy K_{eff} for the $t = 0.45$ nm thick film were deduced from data obtained with thicker films [23]. For $T = 300$ K, we get $A = 1.25$ μerg/cm, an anisotropy field $H_{\text{eff}}^A = 5.3 \pm 0.3$ kOe, and $K_{\text{eff}} = (H_{\text{eff}}^A M_s)/2 = 2.1 \pm 0.3$ Merg/cm^3, which leads to $\epsilon_{\text{el}} = 0.29 \pm 0.04$ μerg/cm. Starting from Eq. (5), and accounting for the values of H_{dep} and T_{dep}, reported in Table I, we estimate $\xi = 19.3$ nm. This value agrees well with the mean lateral size of Pt crystallites ($\sim$10–20 nm) determined by AFM [32] in such a Pt/Co/Pt film supposing a morphological continuity between Pt and Co layers. Therefore, we assume that ξ is temperature independent in the following analysis. We can then estimate the temperature dependence of ϵ_{el}, ϵ_{pin}, Δ, and L_c. $H_{\text{eff}}^A(T)$ is found to be nearly constant over the 50–300 K temperature range, which means that $K_{\text{eff}}(T) \sim M_s(T)$. For $A(T)$, we assumed a temperature variation $\sim M_s(T)^2$. As a result, ϵ_{el} varies as $M_s(T)^{3/2}$ and Δ as $M_s(T)^{1/2}$. This more pronounced temperature variation for ϵ_{el} than for Δ is compatible with the results reported in Figs. 4(a) and 4(b). As expected, Δ decreases when raising the temperature consistently with the found thermal variation of the flow mobility m (Table I). Alternatively, $\epsilon_{\text{el}}(T)$ was deduced from Eq. (5), using the values of M_s, H_{dep} and T_{dep} reported in Table I. As shown in Fig. 4, ϵ_{el} decreases as the temperature increases. The variation is, however, weaker than expected, probably because of the crude assumption: $\Delta \ll \xi$, while both values (7.7 nm and 19.3 nm, respectively) are quite close. The density of pinning energy ϵ_{pin} is
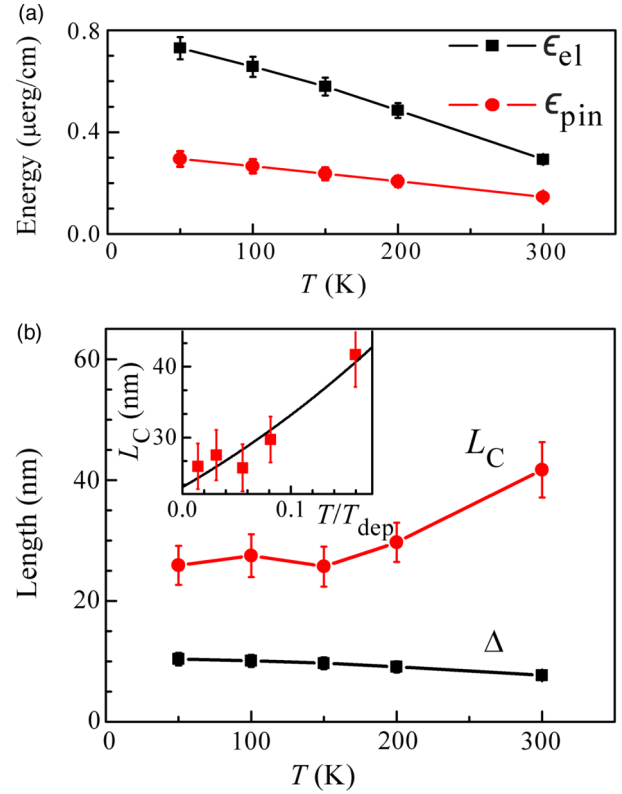

FIG. 4 (color online). (a) Temperature variation of the elastic energy density, ϵ_{el}, and the pinning energy density, ϵ_{pin}. We used the value of $\xi(= 19.3$ nm$)$, obtained for $T = 300$ K. (b) Temperature dependence of the wall width parameter, Δ, and of the Larkin length, L_c. In the inset, L_c is plotted versus T/T_{dep}. The line is the fit of Eq. (8) used for determining the ϕ exponent.

deduced from Eq. (6). Figure 4 shows that ϵ_{pin} exhibits a weaker temperature variation than ϵ_{el}.

Finally, the temperature dependence of the Larkin length, L_c, is calculated from Eq. (7) and the results shown in Fig. 4(b). $L_c(T)$ can be recast in the form [33–35]

$$L_c(T) = L_c^0[1 + (T/T_{\text{dep}})]^{1/\phi}, \qquad (8)$$

where $L_c^0 = L_c(T = 0$ K$)$ and ϕ is the thermal crossover exponent of the Larkin length. Fitting $L_c(T)$ with Eq. (8) [see the inset of Fig. 4(b)] leads to $L_c^0 = 25 \pm 2$ nm and $\phi = 0.24 \pm 0.05$. This last value agrees with the most recent prediction, $\phi = 1/5$ [33–35].

In conclusion, our consistent analysis of the thermal dependence of the field-driven DW motion would be valuably extended to pinning mechanism studies in other systems.

---

*vincent.jeudy@u-psud.fr

[1] P. Chauve, T. Giamarchi, and P. Le Doussal, Phys. Rev. B **62**, 6241 (2000).

[2] M. Müller, D. Gorokhov, and G. Blatter, Phys. Rev. B **63**, 184305 (2001).

[3] S. Brazovskii, and T. Nattermann †, Adv. Phys. **53**, 177 (2004).

[4] T. Giamarchi, *Encyclopedia of Complexity and Science Systems*, Entry 32 (Springer Verlag, Berlin, 2005).

[5] S. Bustingorry, A. B. Kolton, and T. Giamarchi, Europhys. Lett. **81**, 26005 (2008).

[6] A. Kolton, A. Rosso, T. Giamarchi, and W. Krauth, Phys. Rev. Lett. **97**, 057001 (2006); Phys. Rev. B **79**, 184207 (2009).

[7] G. Blatter, V. B. Geshkenbein, A. I. Larkin, and V. M. Vinokur, Rev. Mod. Phys. **66**, 1125 (1994).

[8] W. Kleemann, Annu. Rev. Mater. Res. **37**, 415 (2007).

[9] E. Ferrero, S. Bustingorry, A. B. Kolton, and A. Rosso, C.R. Phys. **14**, 641 (2013).

[10] S. Lemerle, J. Ferré, C. Chappert, V. Mathet, T. Giamarchi, and P. Le Doussal, Phys. Rev. Lett. **80**, 849 (1998).

[11] T. Tybell, P. Paruch, T. Giamarchi, and J.-M. Triscone, Phys. Rev. Lett. **89**, 097601 (2002).

[12] P. Paruch and J.-M. Triscone, Appl. Phys. Lett. **88**, 162907 (2006).

[13] K.-J. Kim, J.-C. Lee, S.-M. Ahn, K.-S. Lee, C.-W. Lee, Y. J. Cho, S. Seo, K.-H. Shin, S.-B. Choe, and H.-W. Lee, Nature (London) **458**, 740 (2009).

[14] J. Ferré, P. J. Metaxas, A. Mougin, J.-P. Jamet, J. Gorchon, and V. Jeudy, C.R. Phys. **14**, 651 (2013).

[15] P. Paruch and J. Guyonnet, C.R. Phys. **14**, 667 (2013).

[16] P. Metaxas, J. Jamet, A. Mougin, M. Cormier, J. Ferré, V. Baltz, B. Rodmacq, B. Dieny, and R. Stamps, Phys. Rev. Lett. **99**, 217208 (2007).

[17] V. Repain, M. Bauer, J.-P. Jamet, J. Ferré, A. Mougin, C. Chappert, and H. Bernas, Europhys. Lett. **68**, 460 (2004).

[18] F. Cayssol, D. Ravelosona, C. Chappert, J. Ferré, and J. Jamet, Phys. Rev. Lett. **92**, 107202 (2004).

[19] P. Metaxas, Solid State Phys. **62**, 75 (2010).

[20] J. Kim, K.-J. Kim, and S.-B. Choe, IEEE Trans. Magn. **45**, 3909 (2009).

[21] S. Emori, and G. S. D. Beach, J. Phys. Condens. Matter **24**, 024214 (2012).

[22] S. Bustingorry, A. B. Kolton, and T. Giamarchi, Phys. Rev. B **85**, 214416 (2012).

[23] See Supplemental Material at http://link.aps.org/supplemental/10.1103/PhysRevLett.113.027205 for details on sample static and dynamics properties.

[24] L. W. Chen and M. C. Marchetti, Phys. Rev. B **51**, 6296 (1995).

[25] M. Feigel'man, V. Geshkenbein, A. Larkin, and V. Vinokur, Phys. Rev. Lett. **63**, 2303 (1989).

[26] T. Nattermann, Phys. Rev. Lett. **64**, 2454 (1990).

[27] P. W. Anderson and Y. B. Kim, Rev. Mod. Phys. **36**, 39 (1964).

[28] A. A. Middleton, Phys. Rev. B **45**, 9465 (1992).

[29] U. Nowak, and K. D. Usadel, Europhys. Lett. **44**, 634 (1998).

[30] S. Bustingorry, A. B. Kolton, and T. Giamarchi, Phys. Rev. E **85**, 021144 (2012).

[31] E. Ferrero, S. Bustingorry, and A. Kolton, Phys. Rev. E **87**, 032122 (2013).

[32] S. Landis, Ph.D thesis, Université Joseph Fourier, Grenoble, France, 2001.

[33] T. Nattermann, Y. Shapir, and I. Vilfan, Phys. Rev. B **42**, 8577 (1990).

[34] S. Bustingorry, P. Le Doussal, and A. Rosso, Phys. Rev. B **82**, 140201 (2010).

[35] E. Agoritsas, V. Lecomte, and T. Giamarchi, Phys. Rev. E **87**, 042406 (2013).